# Enhanced System Robustness of Asynchronous BCI in Augmented Reality Using Steady-State Motion Visual Evoked Potential

Aravind Ravi, *Graduate Student Member, IEEE*, Jing Lu, Sarah Pearce, and Ning Jiang, *Senior Member, IEEE*

***Abstract*— This study evaluated the effect of change in background on steady state visually evoked potentials (SSVEP) and steady state motion visually evoked potentials (SSMVEP) based brain computer interfaces (BCI) in a small-profile augmented reality (AR) headset. A four target SSVEP and SSMVEP BCI was implemented using the Cognixion AR headset prototype. An active (AB) and a non-active background (NB) were evaluated. The signal characteristics and classification performance of the two BCI paradigms were studied. Offline analysis was performed using canonical correlation analysis (CCA) and complex-spectrum based convolutional neural network (C-CNN). Finally, the asynchronous pseudo-online performance of the SSMVEP BCI was evaluated. Signal analysis revealed that the SSMVEP stimulus was more robust to change in background compared to SSVEP stimulus in AR. The decoding performance revealed that the C-CNN method outperformed CCA for both stimulus types and NB background, in agreement with results in the literature. The average offline accuracies for W = 1s of C-CNN were (NB vs. AB): SSVEP: 82% ±15% vs. 60% ±21% and SSMVEP: 71.4% ± 22% vs. 63.5% ± 18%. Additionally, for W = 2s, the AR-SSMVEP BCI with the C-CNN method was 83.3% ± 27% (NB) and 74.1% ±22% (AB). The results suggest that with the C-CNN method, the AR-SSMVEP BCI is both robust to change in background conditions and provides high decoding accuracy compared to the AR-SSVEP BCI. This study presents novel results that highlight the robustness and practical application of SSMVEP BCIs developed with a low-cost AR headset.**

***Index Terms*— Electroencephalography, augmented reality, brain computer interfaces, SSVEP, SSMVEP.**

## I. Introduction

ELECTROENCEPHALOGRAPHY based brain computer interfaces (BCIs) enable humans to establish a direct communication pathway between the brain and the external environment bypassing the peripheral nerves and muscles [1]. Steady state visually evoked potentials (SSVEP) based BCIs are dependent or reactive BCIs that detect the EEG responses to a repetitive visual stimuli with different characteristics (e.g. different frequencies). The BCI can determine which stimulus occupies the user's visual attention by detecting the SSVEP response at the targeted stimulus frequency from the EEG recorded at the occipital and parieto-occipital cortex. This will appear as a significant peak at the targeted stimulus frequency and potentially at its higher order harmonics [2], [3]. The SSVEP stimuli are most commonly designed as a monochromatic object whose intensity is modulated at a fixed frequency, as a result, it appears as a flashing object to the user. This flashing stimulus can induce visual fatigue and discomfort. As a consequence, this decreases the overall signal-to-noise ratio (SNR), decoding performance and interactivity of the BCI. Recently, an extension of the SSVEP BCI known as steady-state motion visually evoked potentials (SSMVEP) based BCI was proposed to address the limitations of the original SSVEP such as fatigue, visual discomfort and relatively low interactive performance of the BCI [4], [5]. Different from the flashing style of SSVEP stimuli, the SSMVEP stimuli are designed as an equal-luminance black and white radial checkerboard. The movement of the checkerboard is modulated at a fixed frequency. Specifically, this movement pattern includes a radial contraction and expansion of the stimulus. SSMVEP BCIs share the advantages of SSVEP BCI such as high SNR, high information transfer rate (ITR) and low participant training time compared to other types of BCIs [6], [7] while minimizing SSVEP-related discomfort for operators.

Traditionally, these stimuli are mostly presented on a computer screen and this limits the application scenario of the system. Moreover, when applied in a real-world environment, the users would need to shift their visual attention back and forth between the stimulus presentation on a monitor and their normal visual field. Recently, affordable virtual reality (VR) and augmented reality (AR) head mounted displays (HMDs), enable the integration of SSVEP BCIs with AR/VR and has gained increased attention [8]–[11]. Furthermore, the minimal setup time and portability of EEG systems make the AR/VR-based BCIs a promising approach to move BCIs out of research lab settings and realize practical real-world applications. Particularly, AR devices allow users to view the

Manuscript received August 11, 2021; revised December 15, 2021; accepted December 28, 2021. Date of publication January 6, 2022; date of current version January 28, 2022. This work was supported in part by the Natural Sciences and Engineering Research Council of Canada (NSERC) Engage-Plus Grant 416317307 and in part by Cognixion Inc. *(Corresponding author: Ning Jiang.)*

This work involved human subjects or animals in its research. Approval of all ethical and experimental procedures and protocols was granted by the University of Waterloo, Office of Research Ethics Under Application No. 31850.

Aravind Ravi, Jing Lu, and Ning Jiang are with the Department of Systems Design Engineering, Waterloo Engineering Bionics Laboratory, University of Waterloo, Waterloo, ON N2L 3G1, Canada (e-mail: ning.jiang@uwaterloo.ca).

Sarah Pearce is with Cognixion Inc., Toronto, ON M5J 2T9, Canada.

Digital Object Identifier 10.1109/TNSRE.2022.3140772

This work is licensed under a Creative Commons Attribution 4.0 License. For more information, see https://creativecommons.org/licenses/by/4.0/

repetitive visual stimuli and the external surroundings in the same field of view providing an enhanced user experience. Several studies have investigated the AR approach based on using a video see-though (VST) based HMD combined with SSVEP BCI [8]–[10]. These studies have applied AR-BCI for applications such as gaming [8], navigation in a 3D space [9], quadcopter control [10], etc. where the real-world scene is acquired using a camera placed on top of the HMD and displayed within the VR environment. The following studies [12], [13] provide a list of other prior work applying similar approaches for other types of BCIs. The VST based HMDs offers only a limited field of view, largely restricted by the camera. Therefore, optical see-through (OST) based HMDs are likely an attractive alternative to the VST-HMDs.

Optical see-through (OST) AR devices consist of a semi-transparent screen or an optical element, and the virtual contents are directly displayed on the screen, overlaid on the user's normal field of view. In [14], the authors implemented a P300 BCI using an OST-HMD based setup. Furthermore, the study compared the results of the online P300 BCI between a computer screen and AR HMD, and reported similar performance in both settings. Recently, a few studies have examined and evaluated the design of SSVEP BCIs in OST-HMD setting [12], [13]. In [12], the authors evaluated the feasibility of SSVEP BCI in an OST-HMD for a robot control and navigation task in a three class SSVEP paradigm. The study implemeted using the Microsoft HoloLens, and assessed the influence of user movement and target display strategies with reported BCI perfomance between 75% and 80%. However, no comparisons with baseline methods such as canonical correlation analysis (CCA) were provided. Users of the Microsoft HoloLens also stated that the HMD felt heavy after a while and they could observe reflections which caused visual discomfort [13].

Another recent study used the Microsoft HoloLens for SSVEP BCI control of a robotic arm, and compared the performance with the same on a computer screen [13]. The study implemented a synchronous eight class SSVEP BCI and reported a performance of 88% in AR compared to 98% on a computer screen. One of the limitations discussed by the authors was related to a dynamically changing surrounding that affected the stability of the SSVEP responses. The authors also observed temporal jitters of event triggers that could impact the performance of synchronous BCI systems.

In a practical condition, it is desirable to enable users to interact with the BCI in an asynchronous manner whenever they want. This means the BCI is not dependent on the precise stimulus timing or predefined time frames [15]. Compared to a cue-paced or synchronous BCI, asynchronous operation requires continuous decoding and analysis of the response. This operation is technically more demanding, but offers a more natural form of interaction. This consists of two states: an intentional control (IC) and a no control (NC) state. For SSVEP/SSMVEP BCIs, the time when the user gazes at the stimulus is called an IC state. The NC state or rest state is defined when the user does not gaze at the stimulus. Recently convolutional neural networks (CNN) based methods are gaining importance in asynchronous classification of SSVEP and SSMVEP BCIs [16]–[18]. These studies have shown that the CNN based methods significantly outperformed the traditional classification methods used for SSVEP classification.

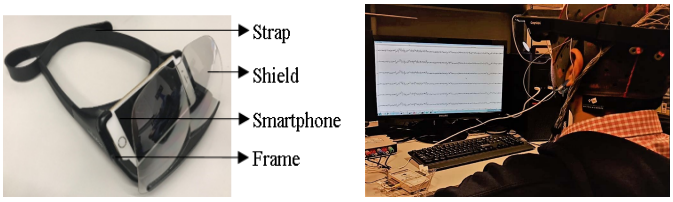


Fig. 1. Experimental setup: a prototype of the Cognixion AR headset and a participant donning the EEG cap with the AR headset.

In the current study, a novel AR-OST based BCI system was proposed and attempted to address some of the above limitations and challenges of current SSVEP systems. A novel low-cost, light weight AR headset was used in this study. The SSVEP and SSMVEP paradigms were compared. Furthermore, a novel experiment methodology was designed that used a stereo video in the background to systematically investigate the effects of the background on the two types of stimuli in an offline analysis. Two types of background conditions were evaluated: an active background (AB) with a stereo video and a non-active (NB) plain black background. A four target SSVEP and SSMVEP BCI was designed. The offline decoding performance of the BCI system was evaluated using the C-CNN method and compared with the baseline CCA method for the data processed in an asynchronous manner. Finally, a pseudo-online analysis was performed to study the asynchronous performance of the SSMVEP BCI.

The remainder of the paper is organized as follows: Section II provides the methodological details of the augmented reality interface, stimulus design, EEG setup, experiment protocol, signal analysis and detection methods. Next, the results of the study are presented in Section III and discussed in Section IV. Finally, Section V concludes the paper and provides directions for future work.

## II. Methodology

### A. Augmented Reality Interface and EEG Setup

In this study, Cognixion's AR headset prototype was used to display the visual stimuli. This is a light-weight optical see-through shield which is partially reflective. The headset is designed so that a smart phone can be securely inserted into its frame and the screen of the phone are reflected on the see-through shield (see Fig. 1). In this study, the visual stimuli were implemented in the smartphone and presented on the screen of the phone, which is in turn presented to the subject through the AR reflective optical shield. All visual stimuli were developed in Unity.

The EEG system consisted of g.USBamp and Gammabox (g.tec Guger Technologies, Austria), and wet electrodes (g.Scarabeo) were used to acquired EEG signal. The sampling rate was 1200 Hz. Three active electrodes were placed over the occipital region: O1, O2, and Oz of the International 10-20 system. FPz was used as the ground and right ear lobe was used as the reference. The AR headset was carefully mounted on the participant over the EEG cap. The experimental setup is illustrated in Figure 1. The details of the complete

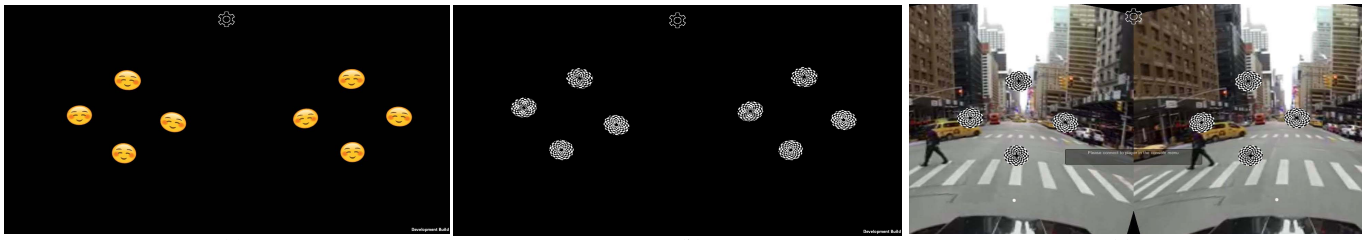

(a) (b) (c)

Fig. 2. Stimulus design – (a) SSVEP stimulus presented on a non-active background, (b) SSMVEP stimulus presented on a non-active background and (c) SSMVEP stimulus presented on an active background (Stereo Video URL: https://youtu.be/2Lq86MKesG4).

experimental protocol will be detailed in subsequent sections. The experimenter synchronized the stimulus presentation on the smartphone and data collection on the PC manually by simultaneously pressing buttons on the PC's keyboard and a remote to control the smartphone app. On the PC, the EEG data was acquired using the OpenViBE software [19] and data analysis was performed offline in Python.

### B. Stimulus Design

Two types of repetitive visual stimuli were compared in this study under two background conditions. These two stimuli were the flashing SSVEP stimulus and the radial checkerboard stimulus. A yellow circular emoji was used to design the flashing SSVEP stimulus. This type of SSVEP stimulus was used to provide more realistic and engaging stimulus compared to the traditional monochromatic colored circular stimulus. Four visual stimuli corresponding to four different flicker frequencies were implemented: 8 Hz, 10 Hz, 12 Hz and 15 Hz. The modulating signal for the stimulation were implemented based on a sequence of alternating ones and zeros as per [20] [21]. This stimulus type will be referred to as emoji or SSVEP stimulus interchangeably in subsequent sections. The stimulus layout is shown in Figure 2.

The second type of visual stimulus was a radial checkerboard SSMVEP stimulus with repetitive motion. The repetitive movement frequencies were: 8 Hz, 10 Hz, 12 Hz and 15 Hz. The checkerboard motion stimulus was implemented as per [4]. This will be referred to as checkerboard/SSMVEP stimulus interchangeably. The stimulus layout was consistent between the SSVEP and SSMVEP stimulus.

Two scenarios were used to simulate active and non-active background conditions. For the active background, a stereo video of an urban setting playing at thirty frames per second was used. The video consisted of a first person view wherein the camera was mounted in the front of a car navigating through the streets of a typical busy North American urban area. The four SSVEP and SSMVEP stimuli were superimposed on the stereo video and presented in the foreground with the video continuously playing in the background. The video also consisted of navigating turns, stops at traffic lights, background sound, and movements or pauses at different points in the video. For both types of stimulus, the starting frame and the ending frame of the background video was kept consistent. For the non-active background, a plain black background was used.

### C. Experiments and Data Collection

Twenty six healthy participants (aged 19-41 years) with normal vision took part in this study. The study received ethics clearance from the University of Waterloo, Office of Research Ethics (ORE: #31850). All participants signed a written informed consent form prior to the start of the experiment. All participants were seated in a comfortable chair facing a plain dark screen throughout the entire duration of the experiment. The experiment room was dimly lit with reduced ambient light. Participants were instructed by the experimenter to avoid any head movements, clenching of the teeth or eye blinks during the experiment. At the start of every session, all visual stimuli in the AR headset were aligned to the center of the field of view of the participant.

This experimental protocol was designed to study the effect of the active and non-active background on the performance of SSVEP and SSMVEP BCI. At the beginning of each trial, one of the four visual stimuli was highlighted in yellow as a cue to direct the user's gaze on the targeted stimulus. The cue would last for 2 s. Next, the participant was asked to gaze at the targeted stimulus for 6 s. Finally, 4 s of break period was provided before the start of the next trial. During the break period, the video would continue to play in the background and the visual stimulus were kept still without movement or flash. Each targeted stimulus was repeated eight times in a pseudorandom order resulting in a total of 32 trials in one session. Each participant performed four sessions, each for one of the four combinations of the two stimulus types (emoji and checkerboard) and two background conditions (active and non-active). The background conditions and stimulus type sequences were also randomized for each participant. Furthermore, participants were provided a break of 2 minutes between two sessions.

### D. Signal Analysis and Detection

Signal analysis was performed offline to assess the effects of the active and non-active backgrounds on the actual responses of the two stimulus types. The data from two participants were rejected due to poor recording quality which likely was a result of mechanical stress from the AR-headset strap on the occipital EEG electrodes. Additional signal quality analysis was performed. The signal-to-noise ratio (SNR) for each participant's data was computed and averaged across trials, stimulus types and background types. Next, those participants' data whose SNR was below the $20^{th}$ percentile of the calculated values

across all participants were rejected. Using this method, data from five participants were removed from further analysis and visual inspection of the spectrum indicated no clear SSVEP or SSMVEP response in the data. The analysis presented in the following sections was performed on data collected from the remaining 19 participants. The influence of the change in background conditions on the frequency responses of the stimuli was assessed using the Fast Fourier Transform (FFT) and SNR for the 6s trials. Canonical correlation analysis (CCA) was used to analyze the strength of the response from the multi-channel EEG data. Finally, the decoding performance of the SSVEP/SSMVEP BCI was evaluated using CCA and Complex-spectrum based Convolutional Neural Networks (C-CNN) [18].

*1) Magnitude Spectrum and Signal-to-Noise Ratio (SNR):* The magnitude spectrum was computed from the FFT of the 6s trials at a resolution of 0.1666 Hz. To compare between stimulus types and background types, the average magnitude spectrum of the four stimulus frequencies (8 Hz, 10 Hz, 12 Hz and 15 Hz) were averaged across all participants, trials and channels (O1, Oz, O2). Next, the SNR was calculated for the fundamental target frequency of each stimulus type from the magnitude spectrum. The SNR for each stimulus frequency $f$ was computed as the ratio of the maximum frequency amplitude in the band [$f - 0.3$ Hz, $f + 0.3$ Hz] to the mean amplitude of the band [$f - 2$ Hz, $f - 0.3$ Hz) and ($f + 0.3$ Hz, $f + 2$ Hz], similar to the method used in [13].

*2) Canonical Correlation Analysis (CCA):* CCA is most widely used as a reference method in the analysis of SSVEP/SSMVEP based BCIs, where the underlying correlation between multi-channel EEG data and a set of reference templates is estimated [4], [16], [22]–[24]. Consider $X$ as the multi-channel EEG signal and $Y$ as the set of reference signals of the same length. Based on the following linear transformations: $x = X^T w_x$ and $y = Y^T w_y$, CCA is used to find the $w_x$ and $w_y$ vectors that maximize the correlation between $x$ and $y$ by solving:

$$\rho(x, y) = max_{w_x, w_y} \frac{\mathrm{E}\left[w_x^T X Y^T w_y\right]}{\sqrt{\mathrm{E}\left[w_x^T X X^T w_x\right] \mathrm{E}\left[w_y^T Y Y^T w_y\right]}}. \quad (1)$$

$$Y_n = \begin{bmatrix} sin(2\pi f_n t) \\ cos(2\pi f_n t) \\ . \\ . \\ sin(2\pi N_h f_n t) \\ cos(2\pi N_h f_n t) \end{bmatrix}, \quad t = \left[\frac{1}{f_s}, \frac{2}{f_s}, \ldots, \frac{N_s}{f_s}\right], \quad (2)$$

where $Y_n \in \mathbb{R}^{2N_h \times N_s}$ are the reference signals, $N_h$ denotes the number of harmonics of the stimulus frequency $f_n$, $N_s$ denotes the number of samples, and $f_s$ denotes EEG sampling frequency. In this study, $N_h = 2$. Finally, the maximum of $\rho$ corresponding to $w_x$ and $w_y$ provides the maximum correlation between the multi-channel EEG and the reference signals. A high value of $\rho$ indicates a strong SSVEP/SSMVEP response present in the multi-channel EEG data. For classification, the canonical features $\rho_{fi}$ were extracted for each segment of the EEG data, and the classification was assigned as: $C = argmax\ (\rho_{fi}), i = 1, 2, 3, 4$.

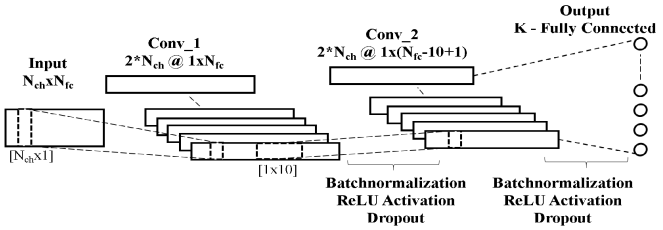


Fig. 3. Convolutional neural network architecture.

In this study, the correlation coefficient was computed on the multi-channel EEG signal to measure the strength of the SSVEP/SSMVEP response. For every trial, the correlation coefficient corresponding to the respective targeted stimulus frequency was computed using the entire 6s duration of the signal. As a result, from the data of each participant in one session, 32 values corresponding to the 32 trials were calculated.

CCA was also used as the benchmark method to evaluate the decoding performance of the SSVEP/SSMVEP BCIs compared in this study. Each trial was preprocessed in an asynchronous manner with a fixed window length (W = [1s, 2s]) and a step size of 0.1 s. The classification accuracy was determined as the stimulation frequency with the maximum CCA correlation coefficient.

*3) Complex Spectrum Features and Convolutional Neural Network (C-CNN):* A recently proposed method called C-CNN outperformed a number of user-dependent training methods for SSVEP BCI and provided higher accuracy for asynchronously processed data than CCA and CNN using magnitude spectrum as input [18], [25]. In this study, the C-CNN method was trained on both the SSVEP and SSMVEP data for stimulus detection.

All trials were processed in an asynchronous manner with a fixed window length (W = [1s, 2s]) and a step size of 0.1 s. Window lengths greater than 2 s were not used as this would considerably affect the speed of the overall BCI system when applied in real-time. The C-CNN is based on the concatenation of the real and imaginary parts of the FFT signal provided as input to the CNN. The network architecture is illustrated in Figure 3. Similar to the previous study [18], [25], the complex FFT of the segmented EEG data was calculated at a resolution of 0.2930 Hz. Next, the real and imaginary frequency components were extracted along each channel and concatenated into a single feature vector as: $I = Re(X)||Im(X)$. As a result, the feature vectors for each channel were stacked one below the other to form the input matrix $I_{C-CNN}$ with dimensions $N_{ch} \times N_{fc}$, where $N_{ch} = 3$ and $N_{fc} = 220$.

$$I_{C-CNN} = \begin{bmatrix} Re\{FFT(x_{O1})\}, & Im\{FFT(x_{O1})\} \\ Re\{FFT(x_{Oz})\}, & Im\{FFT(x_{Oz})\} \\ Re\{FFT(x_{O2})\}, & Im\{FFT(x_{O2})\} \end{bmatrix} \quad (3)$$

This method was trained in a user-dependent scenario, wherein the classifier was trained on data from a single

participant and tested on the data of the same participant. The preprocessing step also provided as a data augmentation strategy to increase number of training examples to train the CNN. An eight-fold stratified cross-validation was performed to evaluate the performance of the classifier such that there were no overlapping samples between the train and validation folds. This is equivalent to a leave one-trial out cross validation. For W = 1s, each fold consisted of 1456 and 208 segments in the training and testing set, respectively. For W = 2s, there were 1176 and 168 segments in the training and testing set, respectively. Furthermore, the CNN was trained individually for a single participant for each stimulus type, background type and window length. The training procedure was similar to the UD-C-CNN training method described in a previous study [18]. The total number of trainable parameters were 5482. The CNN was trained on an Intel Core i5-7200 CPU @ 2.50 GHz and 8 GB RAM. The categorical cross entropy loss was used to train the network. The final parameters of the network were chosen based on the values that provided the highest classification accuracy across participants and were chosen as: $\alpha = 0.001$, $momentum = 0.9$, $D = 0.25$, $L = 0.0001$, $E = 50$, and $B = 64$ where, $\alpha$ was the learning rate, $D$ was the dropout rate, $L$ was the L2 regularization constant, $E$ was the number of epochs and $B$ was the batch size.

### E. Statistical Analysis

Statistical analysis was performed to evaluate the strength of the response measured by the correlation coefficient of CCA for every stimulus frequency. Additional analysis was performed to evaluate the effect of different backgrounds on SSVEP/SSMVEP BCI, using the two decoding methods, CCA and C-CNN.

First, to assess the influence of background conditions on the strength of SSVEP/SSMVEP response, a mixed effects model ANOVA was used. The response variable was the CCA correlation coefficient computed for every trial for the respective targeted stimulus frequency. The participant was a random factor and the following variables were the fixed factors: target frequency with four levels, stimulus type with two levels and background type with two levels. The significance level was fixed as $\alpha = 0.05$.

Next, a mixed-effect model ANOVA was used to analyze the effect of background type on the overall classification accuracy. There were four fixed factors, each with two levels: window length (W = [1s, 2s]), classification method (CCA, C-CNN), stimulus type (SSVEP, SSMVEP), background type (non-active, active). The participant was a random factor and the classification accuracy was the response variable. The null hypothesis was that the classification accuracy was same for all background conditions for both stimulus types. The significance level was fixed as $\alpha = 0.05$.

### F. Asynchronous SSMVEP IC Versus NC Detection

To evaluate the performance of an asynchronous BCI, the data was categorized into two states: an intentional control (IC) state and a no control (NC) state. The 6 s stimulation period was considered as the IC state, and the NC state was defined as the combined duration of the cue and rest period (6 s). This is illustrated in Figure 4. The data was segmented with a fixed window (W = [1s, 2s]) and a step size of 100 ms.

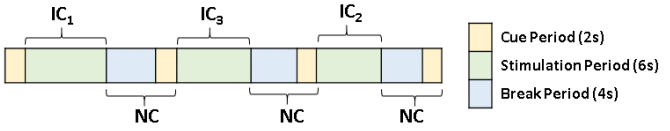


Fig. 4. Asynchronous classification–Intentional control and no control state.

The final softmax layer of the C-CNN architecture was modified to include a fifth NC class, resulting in a total of five neurons: four IC = $(C_1, C_2, C_3, C_4)$ states and one NC = $C_5$ state. The convolutional layers and kernels were kept same as the four-class architecture. An 8-fold cross-validation scheme was used to evaluate the IC vs. NC detection. The network was trained with the categorical cross-entropy loss. The final parameters of the network were chosen as: $\alpha = 0.001$, $momentum = 0.9$, $D = 0.25$, $L = 0.0001$, $E = 80$, and $B = 40$.

### G. Pseudo-Online SSMVEP BCI Performance Evaluation

A two class classification result (IC vs. NC) was deduced from the results of the five class C-CNN. The four target stimuli predictions were combined into a single category IC class, and the rest state/NC was the second class. From the confusion matrices, a true positive (TP) was defined during the IC state when the participant looked at the target and the classifier predicted this segment correctly as an IC state. A false positive (FP) was defined when the classifier predicted a segment as IC when the true label was the NC state. If the classifier misclassified an IC state as NC, this was defined as a false negative (FN). The F1-score and false activation rate (FAR) were calculated as:

$$F1 = \frac{TP}{TP + 0.5 * (FP + FN)} \tag{4}$$

For practical applications, classifying an IC/active state into a different active state usually has more negative effect than classifying it as an inactive class. Therefore, the FAR was defined as the rate of misclassifications within the different IC states, *i.e.* misclassification between one IC state and another IC state. Consider $IC \in \mathbb{R}^{N_c+1 \times N_c+1}$ to be the resultant confusion matrix of the five-class classification, where $N_c = 4$, is the number of IC states. After normalizing the $IC$ by the number of test examples in each class, the FAR per class ($F_j$) was defined as per (5). Finally, the average FAR across all stimulus frequencies was calculated according to (6):

$$F_j = 1 - \frac{IC_{jj}}{\sum_{i=1}^{N_c} IC_{ji}}; \quad j = \{1, 2, \ldots, N_c\} \tag{5}$$

$$\text{FAR} = \frac{1}{N_c} \sum_{j=1}^{N_c} F_j, \quad j = \{1, 2, \ldots, N_c\} \tag{6}$$

The trained five class C-CNN from one of the cross-validation folds was applied in a pseudo-online manner on

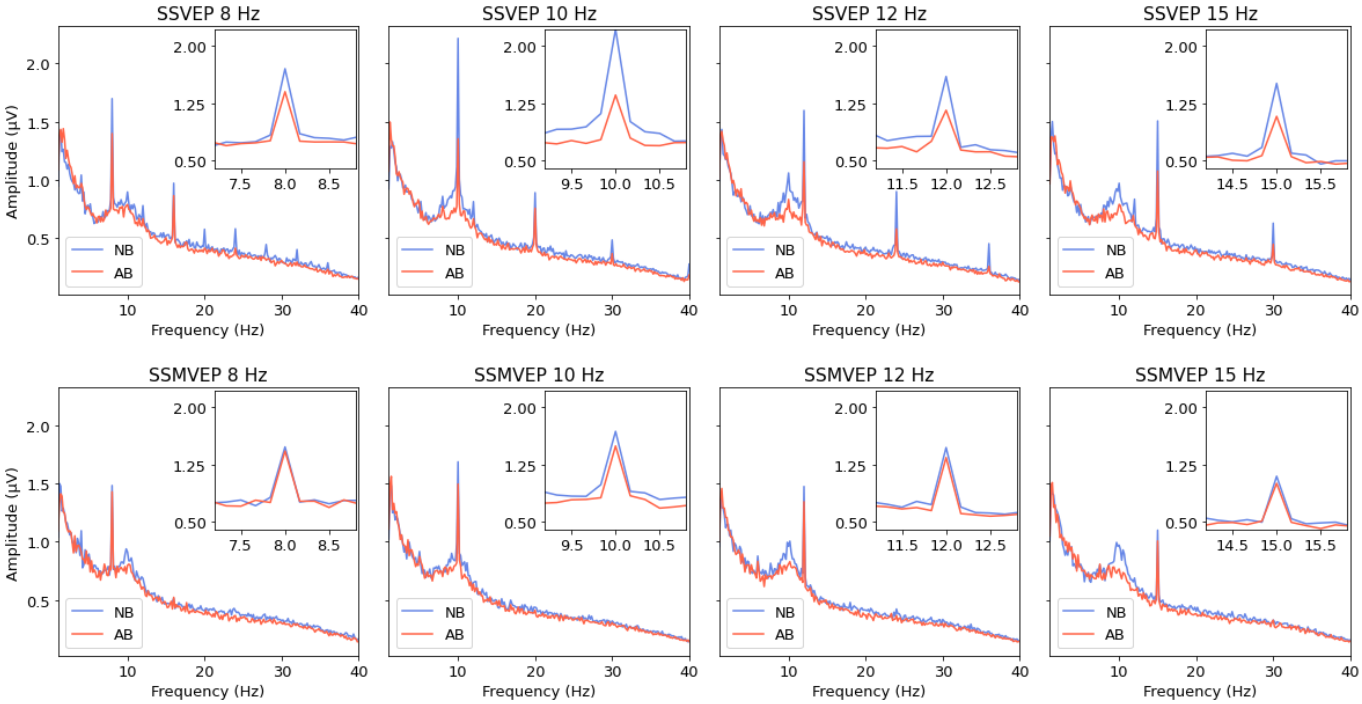


Fig. 5. Average magnitude spectrum of the SSVEP and SSMVEP responses for the four stimulus frequencies (8 Hz, 10 Hz, 12 Hz and 15 Hz) of the 6s trials averaged across all participants, trials and channels (O1, Oz, O2); background– NB (blue) and AB (red).

the entire training session. Specifically, this was applied in a continuous decoding scenario which included segments of data containing the transition segments between IC and NC. This step emulated an online asynchronous BCI.

## III. Results

### A. SSVEP/SSMVEP Response Characteristics

Figure 5 illustrates the average magnitude spectrum of the SSVEP and SSMVEP stimulus under the two background conditions NB and AB. The inserts in the figure shows a magnified version of the fundamental stimulus frequencies. First, the average magnitude spectrum for the SSVEP stimulus clearly indicated the peaks at the targeted fundamental stimulus frequencies and its corresponding harmonics. Next, for the SSMVEP stimulus, a prominent peak at the targeted fundamental frequency was observed for all frequencies, and no other prominent responses were observed. This is in line with the results obtained in previous studies for stimuli presented on a computer screen [4], [26]. These results confirm that the visual stimuli designed for the proposed optical see-through AR system elicits the desired SSVEP and SSMVEP responses.

It can also be observed that the presence of an active background reduced the amplitude of the response at the fundamental frequencies and harmonics for the SSVEP stimulus. The difference in the amplitudes computed between NB and AB for each stimulus frequency were: 0.3 $\mu$V (8 Hz), 0.86 $\mu$V (10 Hz), 0.44 $\mu$V (12 Hz) and 0.43 $\mu$V (15 Hz), respectively. On the other hand, for the SSMVEP stimulus, the difference in amplitudes of the fundamental frequencies between NB and AB were: 0.05 $\mu$V (8 Hz), 0.19 $\mu$V (10 Hz), 0.13 $\mu$V (12 Hz) and 0.09 $\mu$V (15 Hz), respectively. The average reduction in amplitude from NB to AB for all stimulus frequencies were: 28.2% and 8.3% for the SSVEP and SSMVEP responses, respectively. The average SNR across all participants for the SSVEP stimulus for NB vs. AB were (dB): 6.75 vs. 5.43 (8 Hz), 8.15 vs. 5.9 (10 Hz), 6.9 vs. 5.32 (12 Hz) and 8.82 vs. 6.7 (15 Hz). On the contrary, the SNR values for the SSMVEP stimulus were (dB): 5.65 vs. 5.32 (8 Hz), 6.59 vs. 5.77 (10 Hz), 6.11 vs. 6.09 (12 Hz) and 6.02 vs. 6.17 (15 Hz). The average reduction in SNR between NB and AB across all frequencies for SSVEP and SSMVEP were 1.75 dB and 0.25 dB, respectively.

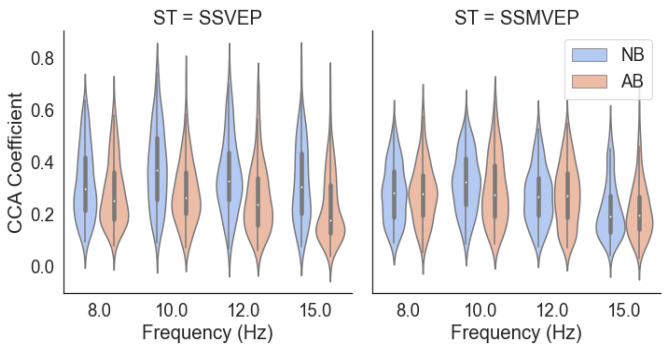


Fig. 6. CCA coefficients computed across participants, for every trial, and each targeted frequency. ST – stimulus type.

### B. CCA Coefficients Analysis

The frequency-specific correlation coefficient for every 6s multi-channel EEG trial was computed based on CCA. Figure 6 summarizes the distribution of the coefficients across

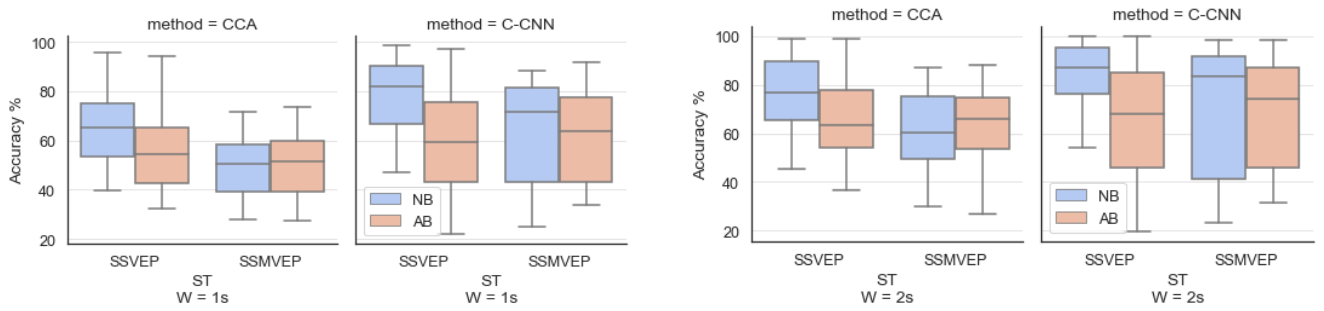


Fig. 7. Four Class BCI Classification Performance - comparison of the classification accuracies across participants for two stimulus types (ST – SSVEP vs. SSMVEP) and background types (NB vs. AB) and data lengths (W = [1s, 2s]).

all participants, target frequencies, stimulus types and background conditions. For the SSVEP/emoji stimulus, active background resulted in consistently lower CCA coefficients than the non-active background across all stimulus frequencies. In contrast, for the SSMVEP/checkerboard stimulus, the magnitude of the CCA coefficients were similar between the two backgrounds across all stimulus frequencies. This result is interesting and not expected, and it indicates that the SSMVEP/checkerboard is less affected by the presence of the active background. For both stimulus types, the response to the 15 Hz stimulus was the lowest among the stimulus frequencies selected for this study and is considerably impacted by the presence of the active background for the SSVEP stimulus.

Statistical analysis of the influence of background type on the stimulus responses revealed that all main effects and two-way interactions were significant ($p \leq 0.01$) and no higher order interaction was significant ($p = 0.107$). Post-hoc analysis with Bonferroni correction was performed to identify pairwise comparisons between the interaction terms, specifically the interaction between the stimulus type and background on the CCA coefficients. For the SSVEP stimulus, there was a significant influence of the change in active versus non-active background ($p < 0.001$). Whereas for the SSMVEP stimulus, there was no significant influence of the change in background on the response/magnitude of CCA coefficients ($p = 1$). These results confirm the observation above: SSMVEP/checkerboard stimulus is more robust and less influenced by the change in background compared to the SSVEP stimulus. Further, frequency specific analysis revealed that, for SSVEP stimulus, the CCA coefficients from the active background were significantly lower than non-active background for 10 Hz, 12 Hz and 15 Hz ($p < 0.001$). Only for the stimulus of 8 Hz, there was no significant difference in CCA coefficients ($p = 0.158$). For the SSMVEP stimulus, on the contrary, no significant effect of background was found for all frequencies ($p = 1$).

### C. Offline 4-Target BCI Classification Results

Figure 7 presents the overall decoding performance of the four target SSVEP/SSMVEP BCIs using the two detection methods. Evidently, the C-CNN outperformed the CCA method for all conditions. For the case of W = 1s, the median

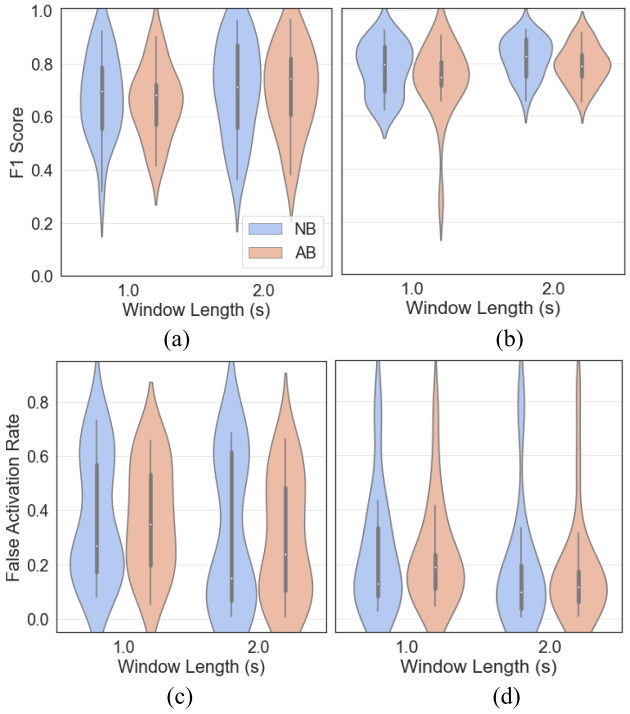


Fig. 8. IC vs. NC detection performance of asynchronous SSMVEP BCI compared between offline (left) and pseudo-online (right) analysis of F1-score (a-b) and False activation rate (c-d).

accuracies of SSVEP-C-CNN decreased 22% from the NB condition to the AB condition (from 82% ± 15% to 60% ± 21%), indicating the performance of SSVEP is significantly affected by the background stimuli. In contrast, the average accuracies of SSMVEP-C-CNN changed less than 8% from the NB condition to the AB condition (from 71.4% ± 22% to 63.5% ± 18%), 2/5 of the change observed in SSVEP. With a wider processing window (W = 2s), the median accuracies of SSVEP-C-CNN decreased approximately 19% from the NB condition to the AB condition (from 86.9% ± 14% to 67.8% ± 24%), while the corresponding accuracy change of SSMVEP-C-CNN was less than 9% (from 83.3% ± 27% to 74.1% ± 22%). The impact of change in background is higher for SSVEP responses compared to SSMVEP. Moreover, the C-CNN results for SSMVEP also illustrate the consistent inter-subject variability compared to SSVEP.

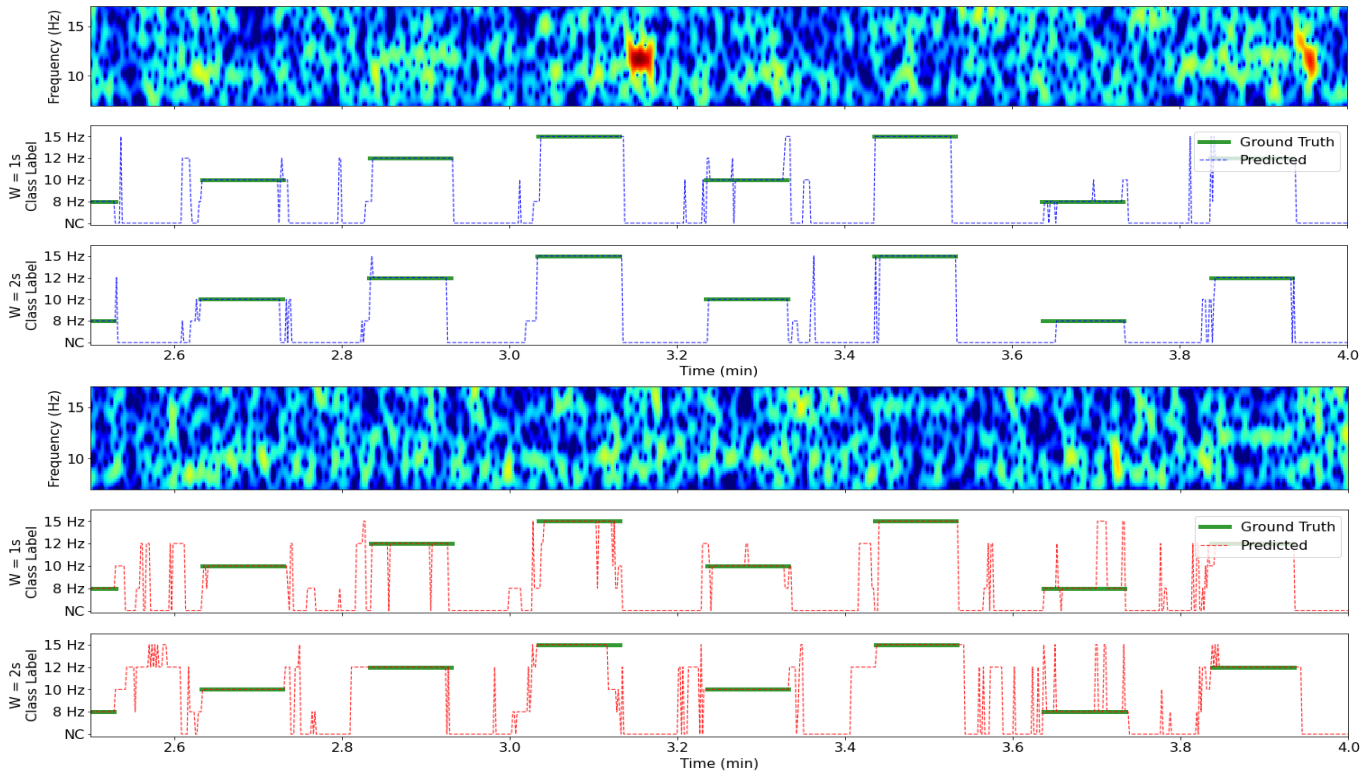


Fig. 9. Temporal evolution of the pseudo-online C-CNN classifier of IC and NC states on a single participant's data for NB (top) and AB (bottom) and W = [1s, 2s]. The average EEG spectrogram computed across channels O1, O2 and Oz; the true and predicted labels.

The above relative higher robustness of SSMVEP over SSVEP is further confirmed by the statistical analysis. The mixed-effects model ANOVA revealed that all main effects were significant ($p < 0.001$). Two-way interactions between stimulus type and background type ($p < 0.001$), and background type and algorithm (p = 0.032) was significant. No other interactions were significant. Post-hoc simultaneous comparisons of the interaction term with Bonferroni correction revealed that for SSVEP stimulus type, the background has a significant effect on the accuracy ($p < 0.001$); for the SSMVEP stimulus type, the influence of the background type was not significant ($p = 1$). Further, there was no significant difference between the SSVEP-AB versus SSMVEP-NB ($p = 1$) and SSVEP-AB versus SSMVEP-AB ($p = 1$) across both detection methods. The C-CNN as significantly higher than CCA under NB condition for both SSVEP (p = 0.013) and SSMVEP (p = 0.016). Again, these results confirmed that the SSMVEP BCI is more robust to changes in background.

### D. Asynchronous IC Vs. NC SSMVEP BCI Results

Figure 8a and 8c illustrate the average offline F1-score and FAR calculated based on the eight-fold cross-validation procedure for the SSMVEP BCI. On the other hand, Figure 8b and 8d illustrate the pseudo-online performance of the SSMVEP BCI calculated on the entire session. The average F1 scores for offline vs. pseudo-online for W = 1s were [NB, AB]: [0.68±0.15, 0.66±0.13] vs. [0.78±0.09, 0.74±0.13], respectively. For W = 2s, offline vs. pseudo-online was [NB, AB]: [0.71±0.17, 0.7±0.16] vs. [0.82±0.07, 0.79±0.07], respectively. As observed previously, the change in background does not influence the F1 score. An average increase of 5% in F1-score can be observed for W = 2s compared to W = 1s. The average FAR for offline vs. pseudo-online for W = 1s were [NB, AB]: [0.36±0.22, 0.37±0.13] vs. [0.24±0.21, 0.23±0.18], respectively. For W = 2s, offline vs. pseudo-online was [NB, AB]: [0.31± 0.27, 0.3±0.22] vs. [0.17±0.2, 0.17±0.2], respectively. An average reduction of 6% in FAR can be achieved for W = 2s compared to W = 1s. The pseudo-online performance was analyzed further.

Figure 9 presents an example of the temporal evolution of the pseudo-online C-CNN predictions on the sessions between 2.5 and 4 minutes from the start of the session. The true and predicted labels are shown along with the average EEG spectrogram calculated across O1, O2 and Oz channels. A high similarity can be observed between the true and predicted labels for both background conditions. For W = 2s, reduced number of false positives and false activations are observed. The misclassifications are mostly observed in the transition regions i.e. at the onset and offset of the stimulation period.

Further investigation was performed to quantify these errors. Two regions were defined: a steady-state (SS) and a transition state (TS) region. The time period between 0.5 s and 5.5 s from the onset and offset of the stimulation period was identified as SS. TS was defined as a 1 s window centered at the onset and offset of the stimulation period. Figure 10 presents the F1-score and FAR calculated in the SS and TS regions. It can be observed that the average FAR is higher in the TS (0.37) compared to the SS (0.18) for all cases. Besides, the average

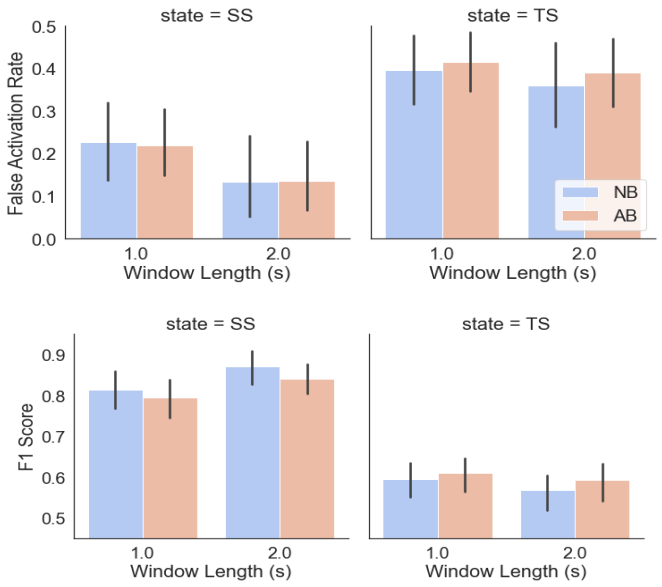


Fig. 10. Pseudo-online transition state (TS) and steady-state (SS): false activation rate (top) and F1-score (bottom).

F1-score was higher in the SS (0.82) compared to the TS (0.6) for W = [1s, 2s] and background conditions.

## IV. Discussions and Conclusion

To the authors' best knowledge, this is the first study to use a novel optical see-through reflective AR headset to present the SSVEP and SSMVEP stimulus. The visual stimuli were presented on the screen of the phone, which was in turn presented to the user through the AR reflective optical shield. It was important to understand and evaluate the EEG responses to the visual stimulus presented in this manner. Evidently, for both SSVEP and SSMVEP stimulus, the spectral analysis revealed the presence of a prominent peak at the fundamental frequency and its harmonics (see Figure 5). Therefore, the proposed AR-OST system is a good candidate for the implementation of SSVEP/SSMVEP BCIs in AR.

The current study investigated the SSVEP/SSMVEP AR-BCI in a complex and dynamically changing background, similar to the operational environment of real-world applications. The results indicated that the presence of the active background in AR, acting as competing stimuli with BCI stimuli, significantly influenced the subjects' responses to both paradigms of visual stimuli, consequently the overall decoding performance of both BCIs. However, it is evident that the SSMVEP stimulus was significantly less affected by the active background than the SSVEP stimulus.

### A. SSVEP/SSMVEP Spectral Analysis

The spectral analysis and CCA coefficient analysis revealed that the reduction in amplitude due to the active background was higher for the SSVEP stimulus (28.2%) compared to the SSMVEP stimulus (8.3%). One of the reasons for the reduction in the amplitude due to the active background could be attributed to the presence of competing stimuli in the background. Previous studies have shown that when multiple flickering visual stimuli are placed in the same visual field, they compete for neural representations. This is called the effect of competing stimuli [27]–[29]. In the current study, we presented a complex and dynamically changing stereo video simultaneously in the background of the SSVEP/SSMVEP stimulus. Therefore, it is possible that various visual elements in the background video interfere or compete for neural representations leading to the decrease in the overall robustness of the SSVEP stimulus. In a recent study, the authors reported a reduction in amplitude of the SSVEP response due to visual distractors compared to no distractors when stimuli were presented on a computer screen [30]. Our analysis provided a similar result for SSVEP stimuli presented on an AR device. On the other hand, there was no reduction in the magnitude of the response for the SSMVEP/checkerboard stimulus when the active background was introduced. This is a particularly interesting result as it shows that the SSMVEP stimulus is more robust even in the presence of competing stimuli in the background.

Next, the reason for the reduction in the amplitude of the response for both stimulus types can be attributed to an increase in visual and mental load in the presence of an active background. A previous study reported that the mental load induced by the flickering stimulus was significantly higher than the checkerboard stimulus [31]. Moreover, the results presented in the current study showed that there was reduction in the SSMVEP amplitude response, but this was not significantly different in the presence of an active competing background. This is likely due to the reduction in attentional demands by the SSMVEP stimulus in general, therefore, leading to higher performance compared to SSVEP stimuli. Another recent study using an optical-see-through HMD, reported a similar result of reduction in the SNR of SSVEP amplitudes in a robotic arm control task and speculated the reason to be due to attention drift in a dynamic background environment[13]. This observation was systematically analyzed and evaluated in our current study. Additionally, we show that the SSMVEP stimulus provides robust offline performance and is less susceptible to change of background conditions.

### B. Four-Class Offline BCI Decoding Performance

The offline decoding performance for the asynchronous four-class AR-SSVEP BCI under the non-active background and 1 second window length was 82% ± 15% with the C-CNN method. This is similar to the previously reported synchronous SSVEP BCI with see-through AR (87.68% ± 7.67%) [13]. In the prior study [13], the dynamic background was a robotic arm control tasks, and the authors' reported an accuracy of 75.55% ± 5.9% with such a dynamic background. In comparison, the accuracy was 67.8% ± 4.8%. Although there are differences such as AR interface, stimulus design, number of stimuli, synchronous versus asynchronous processing and detection methods, the drop in SSVEP performance in the current study was in agreement with the prior study on SSVEP with see-through AR system, confirming the relevance of the current study with respect to the state-of-the-art in the literature. Furthermore, the reduction in performance can be attributed to a lower SNR of the responses when transitioning from a computer screen (CS) to AR interface. A 10% drop

in SSVEP accuracy was reported by a prior study between CS and AR displays[13]. Besides, we observe that including an AB in AR further reduces the overall performance of the SSVEP BCI. This is likely due to the effect of competing stimuli from the AB as explained previous section. Moreover, to the authors' best knowledge, this is the first study to evaluate the SSMVEP BCI performance in AR under changing background conditions. The AR-SSMVEP BCI achieved offline decoding performances of (NB): 71.4% ± 22% and (AB): 63.5% ± 18% for W = 1 s, 83.3% ± 27% (NB) and 74.1% ± 22% (AB) for W = 2 s with the C-CNN method.

### C. Pseudo-Online Asynchronous SSMVEP BCI Performance

The asynchronous pseudo-online SSMVEP BCI using the C-CNN approach can provide high decoding performance that does not require to be precisely synchronized to the onset of the stimulus. Additionally, it was shown to be robust to the change in background conditions. A difference in the performance between the SS and TS was observed which can be attributed to the method of segmentation and training. As these transition windows (TS) were not seen by the classifier at the training phase, these regions were misclassified in the pseudo-online testing phase. The windows in the TS contain a mixture of the SS and TS data, therefore making it a challenge to label such windows. This scenario closely resembles the errors that would likely occur in an online system. One simple solution can be to increase the detection window length, as shown, it can reduce the errors and enhance the overall performance. Future studies can investigate other methods to enhance the TS performance.

### D. Practical Considerations

This study evaluated the AR-SSVEP/SSMVEP BCI system based on practical considerations. The stereo video or dynamically changing environment, which was presented with the optical see-through HMD, was selected to simulate real-life environmental conditions as much as possible, given a laboratory setting. Furthermore, the novel optical-see through HMD used in this study was the AR headset prototype by Cognixion which is relatively low-cost and easy to use compared to other AR HMD devices [13]. A stimulus such as the SSMVEP stimuli, which causes less visual fatigue, is shown to be robust against active backgrounds. The minimal BCI system design with only three EEG channels O1, O2, Oz, and short experimental protocol offers a fast and simple setup and calibration. Future studies can also explore the performance of the presented system in an online SSMVEP BCI setting under different dynamic background conditions.

### E. Conclusion

In this study, in-depth analysis and comparisons of SSVEP and SSMVEP responses in AR were performed under two types of background conditions: a non-active plain black background (NB) and an active background (AB). The results of the analysis clearly demonstrated that the SSMVEP is more robust than SSVEP in the presence of dynamic background stimuli. This feature of SSMVEP is a key advantage when considering practical application of BCIs, and can provide a high and consistent decoding performance when deployed with an affordable OST-AR headset. The simple design, small profile, low setup complexity, short calibration time, and high decoding performance positions the proposed system as an attractive reactive BCI for practical applications. In conclusion, this study serves as a key extension to the current literature on SSVEP and SSMVEP BCIs in AR, and provide novel approaches to support prospective BCI paradigms and system designs.

## Acknowledgment

The authors thank all the participants who took part in this study. The authors thank the anonymous reviewers for their valuable feedback and suggestions.

## References

[1] J. Wolpaw, N. Birbaumer, D. McFarland, G. Pfurtscheller, and T. Vaughan, "Brain-computer interfaces for communication and control," *Clin. Neurophys.*, vol. 113, no. 6, pp. 767–791, 2002.

[2] C. S. Herrmann, "Human EEG responses to 1–100 Hz flicker: Resonance phenomena in visual cortex and their potential correlation to cognitive phenomena," *Exp. Brain Res.*, vol. 137, nos. 3–4, pp. 346–353, Apr. 2001.

[3] Y. Wang, R. Wang, X. Gao, B. Hong, and S. Gao, "A practical VEP-based brain-computer interface," *IEEE Trans. Neural Syst. Rehabil. Eng.*, vol. 14, no. 2, pp. 234–239, Jun. 2006.

[4] W. Yan *et al.*, "Steady-state motion visual evoked potential (SSMVEP) based on equal luminance colored enhancement," *PLoS ONE*, vol. 12, no. 1, pp. 1–18, 2017.

[5] X. Han *et al.*, "Comparison of visual cortex functional connectivity patterns based on steady-state monochromatic flicker and oscillating checkerboard visual stimulus," in *Proc. 15th Int. Conf. Ubiquitous Robots (UR)*, Jun. 2018, pp. 732–736.

[6] B. Allison, T. Lüth, D. Valbuena, A. Teymourian, I. Volosyak, and A. Gräser, "BCI demographics: How many (and what kinds of) people can use an SSVEP BCI?" *IEEE Trans. Neural Syst. Rehabil. Eng.*, vol. 18, no. 2, pp. 107–116, Apr. 2010.

[7] C. Guger *et al.*, "How many people could use an SSVEP BCI?" *Frontiers Neurosci.*, vol. 6, pp. 2–7, Nov. 2012.

[8] B. Koo, H.-G. Lee, Y. Nam, and S. Choi, "Immersive BCI with SSVEP in VR head-mounted display," in *Proc. 37th Annu. Int. Conf. IEEE Eng. Med. Biol. Soc. (EMBC)*, Aug. 2015, pp. 1103–1106.

[9] J. Faller *et al.*, "A feasibility study on SSVEP-based interaction with motivating and immersive virtual and augmented reality," 2017, *arXiv:1701.03981*.

[10] M. Wang, R. Li, R. Zhang, G. Li, and D. Zhang, "A wearable SSVEP-based BCI system for quadcopter control using head-mounted device," *IEEE Access*, vol. 6, pp. 26789–26798, 2018.

[11] D. Wen, B. Liang, Y. Zhou, H. Chen, and T.-P. Jung, "The current research of combining multi-modal brain-computer interfaces with virtual reality," *IEEE J. Biomed. Health Informat.*, vol. 25, no. 9, pp. 3278–3287, Sep. 2021.

[12] H. Si-Mohammed *et al.*, "Towards BCI-based interfaces for augmented reality: Feasibility, design and evaluation," *IEEE Trans. Vis. Comput. Graphics*, vol. 26, no. 3, pp. 1608–1621, Mar. 2020.

[13] Y. Ke, P. Liu, X. An, X. Song, and D. Ming, "An online SSVEP-BCI system in an optical see-through augmented reality environment," *J. Neural Eng.*, vol. 17, no. 1, Feb. 2020, Art. no. 016066.

[14] K. Takano, N. Hata, and K. Kansaku, "Towards intelligent environments: An augmented reality–brain–machine interface operated with a see-through head-mount display," *Frontiers Neurosci.*, vol. 5, pp. 1–5, Apr. 2011.

[15] G. R. Müller-Putz and G. Pfurtscheller, "Control of an electrical prosthesis with an SSVEP-based BCI," *IEEE Trans. Biomed. Eng.*, vol. 55, no. 1, pp. 361–364, Jan. 2008.

[16] X. Zhang *et al.*, "A convolutional neural network for the detection of asynchronous steady state motion visual evoked potential," *IEEE Trans. Neural Syst. Rehabil. Eng.*, vol. 27, no. 6, pp. 1303–1311, Jun. 2019.

[17] N. Waytowich *et al.*, "Compact convolutional neural networks for classification of asynchronous steady-state visual evoked potentials," *J. Neural Eng.*, vol. 15, no. 6, Dec. 2018, Art. no. 066031.

[18] A. Ravi, N. H. Beni, J. Manuel, and N. Jiang, "Comparing user-dependent and user-independent training of CNN for SSVEP BCI," *J. Neural Eng.*, vol. 17, no. 2, 2020, Art. no. 026028.

[19] Y. Renard *et al.*, "OpenViBE: An open-source software platform to design, test, and use brain–computer interfaces in real and virtual environments," *Presence*, vol. 19, no. 1, pp. 35–53, Feb. 2010.

[20] Y. Wang, Y.-T. Wang, and T.-P. Jung, "Visual stimulus design for high-rate SSVEP BCI," *Electron. Lett.*, vol. 46, no. 15, p. 1057, 2010.

[21] M. Nakanishi, Y. Wang, Y.-T. Wang, Y. Mitsukura, and T.-P. Jung, "Generating visual flickers for eliciting robust steady-state visual evoked potentials at flexible frequencies using monitor refresh rate," *PLoS ONE*, vol. 9, no. 6, Jun. 2014, Art. no. e99235.

[22] Z. Lin, C. Zhang, W. Wu, and X. Gao, "Frequency recognition based on canonical correlation analysis for SSVEP-based BCIS," *IEEE Trans. Biomed. Eng.*, vol. 54, no. 6, pp. 1172–1176, Jun. 2007.

[23] M. Nakanishi, Y. Wang, Y. Te Wang, and T. P. Jung, "A comparison study of canonical correlation analysis based methods for detecting steady-state visual evoked potentials," *PLoS ONE*, vol. 10, no. 10, pp. 1–18, 2015.

[24] G. Bin, X. Gao, Z. Yan, B. Hong, and S. Gao, "An online multi-channel SSVEP-based brain–computer interface using a canonical correlation analysis method," *J. Neural Eng.*, vol. 6, no. 4, Aug. 2009, Art. no. 046002.

[25] A. Ravi, N. Heydari, and N. Jiang, "User-independent SSVEP BCI using complex FFT features and CNN classification," in *Proc. IEEE Int. Conf. Syst., Man Cybern. (SMC)*, Oct. 2019, pp. 4175–4180.

[26] W. Yan, G. Xu, J. Xie, M. Li, and Z. Dan, "Four novel motion paradigms based on steady-state motion visual evoked potential," *IEEE Trans. Biomed. Eng.*, vol. 65, no. 8, pp. 1696–1704, Aug. 2018.

[27] K. B. Ng, A. P. Bradley, and R. Cunnington, "Effect of competing stimuli on SSVEP-based BCI," in *Proc. Annu. Int. Conf. IEEE Eng. Med. Biol. Soc. (EMBS)*, Aug. 2011, pp. 6307–6310.

[28] A. Ravi, J. Manuel, N. Heydari, and N. Jiang, "A convolutional neural network for enhancing the detection of SSVEP in the presence of competing stimuli," in *Proc. 41st Annu. Int. Conf. IEEE Eng. Med. Biol. Soc. (EMBC)*, Jul. 2019, pp. 6323–6326.

[29] A. Ravi, S. Pearce, X. Zhang, and N. Jiang, "User-specific channel selection method to improve SSVEP BCI decoding robustness against variable inter-stimulus distance," in *Proc. 9th Int. IEEE/EMBS Conf. Neural Eng. (NER)*, Mar. 2019, pp. 283–286.

[30] R. Zerafa, T. Camilleri, K. P. Camilleri, and O. Falzon, "The effect of distractors on SSVEP-based brain-computer interfaces," *Biomed. Phys. Eng. Exp.*, vol. 5, no. 3, Apr. 2019, Art. no. 035031.

[31] J. Xie, G. Xu, J. Wang, M. Li, C. Han, and Y. Jia, "Effects of mental load and fatigue on steady-state evoked potential based brain computer interface tasks: A comparison of periodic flickering and motion-reversal based visual attention," *PLoS ONE*, vol. 11, no. 9, pp. 1–15, 2016.